ELSEVIER

Chemical Engineering Journal 140 (2008) 287–295

Chemical Engineering Journal

www.elsevier.com/locate/cej

Kinetic modelling of methylcyclohexane ring-opening over a HZSM-5 zeolite catalyst

Pedro Castaño [a,*], Ana G. Gayubo [a], Barbara Pawelec [b], José Luis G. Fierro [b], José Maria Arandes [a]

[a] *University of the Basque Country, Department of Chemical Engineering, PO Box 644, E-48080 Bilbao, Spain*

[b] *Institute of Catalysis and Petrochemistry, CSIC, C/ Marie Curie, 2 Cantoblanco, E-28049 Madrid, Spain*

Received 4 July 2007; received in revised form 14 September 2007; accepted 19 September 2007

Abstract

A kinetic model is proposed in order to quantify product distribution in the ring-opening (using high hydrogen concentration in the reaction medium) of methylcyclohexane (MCH) over a catalyst based on HZSM-5 zeolite. The model is based on a reaction scheme proposed by Cerqueira et al. for methylcyclohexane cracking at atmospheric pressure, which has been modified in order to include the effect of hydrogen over the individual reaction steps. The experimental results used for estimating the kinetic constant were obtained in a fixed bed isothermal reactor in a wide range of conditions, i.e. 250–450 °C; WHSV = 0.5–10.5 h^{-1} (τ = 0.095–2 g_{cat} h $g_{MCH}{}^{-1}$); pressure = 5–80 bar; H_2/MCH molar flow ratio = 4–79; conversion = 0–100%. The kinetic model proposed can be regarded as a basis for the proposal of models for ring-opening reactions of more complex naphthenic feedstock from a prior hydrogenation step involving aromatic refinery streams of secondary interest.

Keywords: Kinetic model; Hydrocracking; HZSM-5 zeolite; Cycloalkane; Naphthene ring-opening

1. Introduction

The trend in the market evolution of refinery products requires greater production of light olefins, whose demand is increasing due to their use as raw materials in the production of plastics. The greater production of these streams also leads to an increase in the production of streams of secondary interest and, particularly, of aromatic ones [1].

Amongst the alternatives for the transformation of aromatics into streams of commercial interest, hydrotreatment is a versatile process with increasing implementation in refineries [2,3]. The process may be carried out in a single step of hydrocracking (HYC) or in two steps in series, the first being hydrogenation (HYD) and the second one the ring-opening of the naphthenes produced in the first step. This two-step route has been studied in detail by Weitkamp et al. [4] as an integrated process in the steam cracker, with the aim of transforming pyrolysis gasoline (PyGas, secondary interest stream because of its high aromatic content) into C_{2+} *n*-alkanes, which are an optimum feedstock for returning to the steam cracker unit [5]. In the ARINO® (Aromatic RINg Opening) two-step process, naphthene conversion and the composition of the product stream, which should be constituted mainly by isoalkanes or C_{2+} *n*-alkanes, are a consequence of the operating conditions of the second step (ring-opening) and of the acidity of the catalyst (prepared based on a HZSM-5 zeolite) [6–8].

Methylcyclohexane has been extensively adopted in literature as a model molecule in the cracking of naphthenes with [6,9,10] and without [11–13] hydrogen, using in the latter similar conditions as in the FCC unit. Indeed, MCH is a product of toluene hydrogenation, which is the component in the BTX (benzene, toluene and xylenes) with higher surplus foreseen and lower hydrogenation rate compared with benzene.

The cracking of MCH is an irreversible endothermic reaction that is favoured by increasing temperature, hydrogen partial pressure and catalyst acidity [4,7,12]. In the presence of hydrogen, HZSM-5 zeolite activates the intervention of hydrogen in the cracking mechanisms by promoting non-classical (Haag

* Corresponding author. Current address: Delft University of Technology, Department of Catalysis Engineering, Netherlands. Tel.: +34 94 6012511; fax: +34 94 6013500.

E-mail address: p.castano@tudelft.nl (P. Castaño).

1385-8947/$ – see front matter © 2007 Elsevier B.V. All rights reserved.
doi:10.1016/j.cej.2007.09.041

Nomenclature

CMR	cracking mechanism ratio, Eq. (3)
E_i	activation energy of step i in Fig. 5
F_{calc}, F_{exp}	value of the objective function, Eq. (9)
k_i	kinetic constant of step i in Fig. 5
m_i	mass flow-rates of lump or compound i, kg s^{-1}
N_{exp}	number of experiments, Eq. (9)
P_i	partial pressure of compound i, bar
Q_{hc}^{in}, Q_{hy}^{out}	mass flow of hydrocarbons in the reactor inlet and outlet, kg s^{-1}
SSR	sums of squared residuals of regression, Eq. (9)
WHSV	weight hourly space velocity, h^{-1}
x_i	mass fraction of lump or compound i, $g_i\ g_{total}^{-1}$
X	conversion of MCH (%)
y_i	mass fraction of lump or compound i, $g_i\ g_{hc}^{-1}$
Y_i	yield of lump or compound i, see Eq. (2), wt%

Greek letters

α	hydrogen reaction order
δ	parameter of correction of the mass balance, Eq. (1)
τ	space time, $g_{cat}\ h\ g_{MCH}^{-1}$

Subscripts

A, C, I, P, M, H_2	aromatics, cycloalkanes, isoalkanes, paraffins (C_{2+} *n*-alkanes), methane and hydrogen
C_1, C_2, iC_4	methane, ethane, isobutane
MCH, cat	methylcyclohexane and catalyst

Dessau or protolytic-scission of a carbonium ion) and classical mechanism (hydride transfer step to a carbenium ion followed by β-scission). The protolytic cracking is the prevailing mechanism promoted by HZSM-5 zeolite without hydrogen [14,15] while classical cracking has a smaller relevance in the absence of hydrogen on a HZSM-5 zeolite than on a HY zeolite due to steric restrictions (two molecules are required). On the other hand, oligomerization-cracking mechanism is expected to be unfavourable under a high hydrogen partial pressure due, firstly, to the dilution of the reactant and, secondly, to the hydrogenation of the alkenes generated in the cracking by β-scission. The global effect should explain both the increase in cracking activity and the increase in the yield of alkenes over that corresponding to hydrogen-free cracking as determined in literature [7].

The aim of this paper is to propose a kinetic model for the cracking of naphthenes, which is carried out with hydrogen in the reaction medium (protolytic- and β-scission in the presence of hydrogen). Methylcyclohexane (MCH) has been taken as model reactant since the reactivity of this compound is similar to other naphthenes in catalytic cracking while HZSM-5 zeolite exhibit enhanced selectivity of C_{2+} *n*-alkanes [16]. Besides, the proposed kinetic model can be regarded as a tool for understanding the mechanisms of scission in hydrocracking conditions over the acid sites.

2. Procedures

2.1. Catalyst

The catalyst has been prepared from a HZSM-5 zeolite provided by Zeolyst International in ammonia form, with an atomic ratio Si:Al = 15 (SiO_2:Al_2O_3 = 30; Na_2O = 0.05 wt%). The zeolite (25 wt%) was agglomerated with: (i) bentonite (30 wt%) as binder (montmorillonite-type clay without catalytic activity), which provides the agglomerate with mechanical resistance to abrasion, attrition and erosion, for withstanding the high pressures required during reaction, and (ii) an inert charge of α-Al_2O_3 (Merck) (45 wt%) to increase the stability of the crystal array and thermal conductivity. The agglomeration provides the catalyst with particle mesopores corresponding to the bentonite and alumina, and also macropores or cavities between the microparticles of the individual components. The final catalytic particles have been obtained after humid extrusion, drying (24 h at 120 °C), sieving in the 0.15–0.30 mm range and activation through calcination (3 h at 550 °C), in order to attain a suitable control of dehydroxylation by creating the acid sites (Brönsted and Lewis) responsible for cracking. The selection of a low Si:Al atomic ratio in the original zeolite gives way to a zeolite with high acidity, as required in severe ring-opening [6,8].

The main physical properties of the catalyst, measured by N_2 adsorption–desorption in a Micromeritics ASAP 2010 apparatus are: BET surface area, 220 $m^2\ g_{cat}^{-1}$; pore volume, 0.092 $cm^3\ g_{cat}^{-1}$; micropore volume, 0.040 $cm^3\ g_{cat}^{-1}$. Total acidity, measured by TPD of ammonia (in a Setaram TG-DSC 111 equipped on-line with a Balzers Quastard 422 mass spectrometer) at 150 °C is 175 $\mu mol_{NH3}\ g_{cat}^{-1}$, which coincides with that obtained with the same equipment by combining the thermogravimetric and calorimetric measurements of NH_3 differential adsorption [17,18]. This latter technique also records a uniform distribution of acid sites with an average strength of 152 J $(mmol_{NH3})^{-1}$. The Brönsted to Lewis acid site molar ratio, obtained in a FTIR spectrophotometer (Nicolet 740 SX), from the vibrational bands of adsorbed pyridine at 1547 and 1453 cm^{-1} at 150 °C, is 2.62.

2.2. Reaction and analysis equipment

The reaction unit (Fig. 1) may operate up to 100 bar and 500 °C and has the following components:

(i) *Gas feeder*. With four individual lines (0–100 bar) provided with an anti-return valve, a cut valve and a mass flow-meter (Bronkhorst High-Tech B.V.) actuated by a PID controller. The four lines end in a line supplied with a pressure meter (EL-PRESS; Bronkhorst High-Tech B.V.).

(ii) *Liquid feeder*. The liquid reactant is stored in a 500 mL vessel and is fed by a piston pump (Gilson 307) provided with a 5SC head. This system allows for operating with flow-rates between 0.010 and 5 mL min^{-1}, up to a pressure of 600 bar and temperatures in the 0–40 °C range.

(iii) *Reactant mixer and preheater*. The gas and/or liquid feeds are mixed and preheated by convection in an electric oven

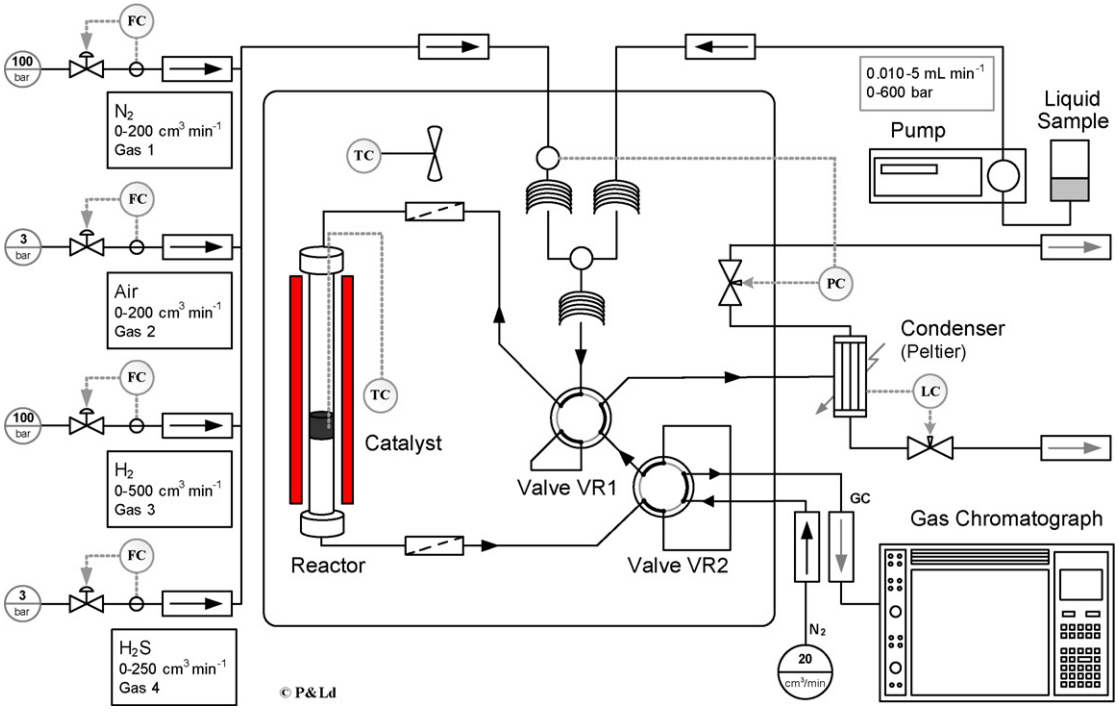

Fig. 1. Scheme of the reaction equipment. Keys: FC: flow controller; PC: pressure controller; TC: temperature controller, LC: level controller; GC: gas chromatograph.

provided with a K-type thermocouple and a PI temperature controller.

(iv) *Reactor*. The reactor is a downflow fixed bed consisting of a stainless steel cylindrical tube with 8 mm internal diameter and 303 mm height. The catalyst is supported on a porous plate (Incoloy) of 2 mm thickness placed at 128 mm from the base of the reactor. The feed at the inlet is regulated by a Valco valve. Temperature is measured with a K-type thermocouple connected to a PID controller, which operates the resistances placed in the reactor jacket.

(v) *Product analysis*. The products that leave the reactor pass through a filter and subsequently through a six-port Valco valve (VR2), where they fill a loop and are entrained by a N_2 stream of 20 $cm^3\ min^{-1}$ to a gas chromatograph (GC). The apparatus used for analysis is a GC Hewlett Packard 5890 Series II equipped with a flame ionization detector (FID) and a capillary column, Tracer TRB-1, filled with methylsilicon and of 60 m length, 0.20 mm internal diameter and 0.5 μm thickness on the wall. Given that the integrated area obtained from the FID considers only the hydrocarbon stream (hydrogen is not analysed), the conversion at the outlet has been calculated by carbon mass balances in the reactor inlet and outlet streams. The identification of the reaction products has been carried out with a Hewlett Packard 5989B mass spectrometer on-line with a Hewlett Packard 5890 Series II Plus gas chromatograph provided with the same column as those used in product analysis.

(vi) *Conditioning of the outlet stream*. The heavier products are separated in a condenser (Peltier cell) at 0 °C, which is equipped with a level measurement device. The liquid stream is depressurized and collected in a vessel. Depressurization is carried out by means of a needle valve actuated by a PID controller and by closing the control loop with the level meter in the Peltier cell. The gaseous stream again enters the oven in order to be reheated and depressurized. On this occasion, depressurization is now attained by a needle valve actuated by a PID pressure controller and the control loop is closed by the inlet pressure meter.

2.3. Reaction conditions

Kinetic runs have been conducted under the following conditions: temperature = 250–450 °C; WHSV = 0.5–10.5 h^{-1} (τ = 0.095–2 $g_{cat}\ h\ g_{MCH}{}^{-1}$); pressure = 5–80 bar; $mol_{H_2}\ mol_{MCH}{}^{-1}$ = 4–79; conversion = 0–100% (integral reactor); time on stream (TOS) = 0–7 h. The total number of runs was 356 under 178 experimental conditions. All runs have been repeated in order to attain suitable statistical significance.

2.4. Parameter estimation

The products detected in MCH transformation have been grouped into methane, C_{2+} *n*-alkanes, isoalkanes, cycloalkanes (excluding MCH) and aromatics. The main compounds of each lump (excluding methane) are: C_{2+} *n*-alkanes; propane and ethane. Isoalkanes; isobutanes and isopentanes at 350 °C and isohexanes at 250 °C. Cycloalkanes; methyl and ethylcyclopentanes. Aromatics: toluene, benzene and xilenes.

The use of lumps of components is a well-known procedure in the cracking processes when the aim is to obtain a kinetic model for use in the reactor design [19]. The kinetic models obtained using lumping have a good balance concerning rigour and simplicity, and are useful for predicting the main effects of operating variables on the interesting products, which are those

that quantify their quality and properties of the products [20]. Moreover, the number of kinetic constants is limited and, hence, they can be accurately calculated. It is noteworthy that, under the conditions studied, no alkenes are detected in the product stream, which is evidence of the hydrogenating capacity of the HZSM-5 zeolite [21].

In order to close the mass balance, the mass flow-rate of hydrocarbons at the outlet (Q_{hc}^{out}) has been considered to be higher than that at the inlet (Q_{hc}^{in}) due to the incorporation of H_2 into the stream. The experimental value of parameter δ has been used to consider this fact:

$$\delta = \frac{Q_{hc}^{in}}{Q_{hc}^{out}} \quad (1)$$

The yield of the i product (Y_i) has been defined as the ratio between the mass flow-rate of such i product and the mass flow-rate of MCH in the feed, corrected for the incorporation of H_2 into the hydrocarbon stream with the parameter mentioned above (δ):

$$Y_i = \frac{m_i}{(m_{MCH})_0}\delta \quad (2)$$

The conversion of MCH has been calculated by the sum of the yields of products (every compound detected in the GC except MCH) while the selectivity of each i product is the ratio between the corresponding yield and the sum of product yields. The cracking mechanism ratio (CMR) index has been used to quantify the significance of protolytic cracking over the complete reaction mechanism, and this parameter is calculated as follows [4,22]:

$$CMR = \frac{Y_{C_1} + Y_{C_2}}{Y_{iC_4}} \quad (3)$$

where Y_i are the yields of C_1 (methane), C_2 (ethane) and iC_4 (isobutane). The formation of methane and ethane is attributed to protolitic-scission of a carbonium ion (RH_2^+) while the production of isobutane comes mainly form isomerisation/β-scission of a carbenium ion (R^+), thus CMR is a ratio which compares the incidence of monomolecular over bimolecular cracking.

The kinetic constants, the activation energies and the reaction orders have been calculated by fitting the experimental concentrations x_i to the values calculated by numerical integration of differential rate equations using Matlab R14 routines. The numerical integration of these equations has been carried out by using ode15s and ode45 codes, while the minimization of errors by the lsqcurvefit function, which uses the large-scale algorithm, subspace trust region method based on the interior-reflective Newton method, to solve nonlinear curve-fitting problems in the least-squares sense:

$$SSR = \sum_{i=1}^{N_{exp}} (F_{calc}(k, x_i) - F_{exp})^2 \quad (4)$$

3. Results and discussion

3.1. Previous analysis of data

The low catalytic activity of the agglomerate and inert material has been checked under the same reaction conditions used with the catalyst based on HZSM-5 zeolite. The conversion of MCH is lower than 1% under the more severe conditions, due to the low concentration and strength of the binder acid sites, measured by NH_3-DSC (concentration <50 $\mu mol_{NH3}\ g_{cat}^{-1}$ and strength <40 J $mmol_{NH3}^{-1}$).

An analysis of the effect of certain operating conditions characteristic to ring-opening has been carried out in order to shed light for the proposal of a kinetic scheme. Fig. 2 shows the effect of hydrogen partial pressure on the conversion of methylcyclohexane, for different values of space time. Although the total pressure (sum of MCH and hydrogen partial pressure) increase together with the hydrogen partial pressure, the results reported here are analogous to the ones using the same total pressure and increasing hydrogen partial pressure (adding an inert gas) as we reported earlier [16].

The results presented in Fig. 2, corresponding to 350 °C, show that hydrogen promotes ring scission rate, i.e. as hydrogen partial pressure is increased, so do the rates of endocyclic cracking and those of exocyclic cracking and isomerization, being reflected in a higher yield and selectivity concerning methane, C_{2+} n-alkanes and, especially, isoalkanes.

As is observed in Fig. 2, 100% conversion is reached for WHSV = 1 h^{-1} (on the basis of pure zeolite; WHSV = 4 h^{-1}) under a hydrogen partial pressure higher than 39 bar. This result

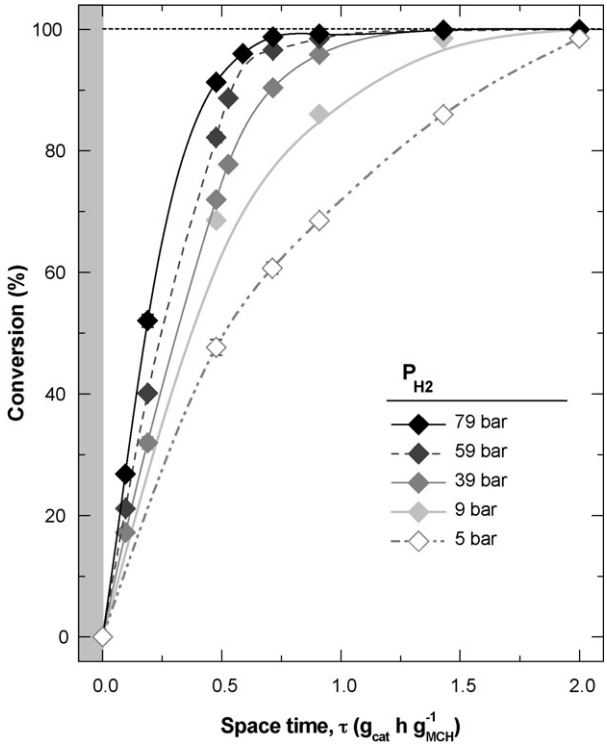

Fig. 2. Effect of hydrogen partial pressure on the evolution of conversion with space time. P_{MCH} = 1 bar, $P = P_{MCH} + P_{H_2}$, 350 °C.

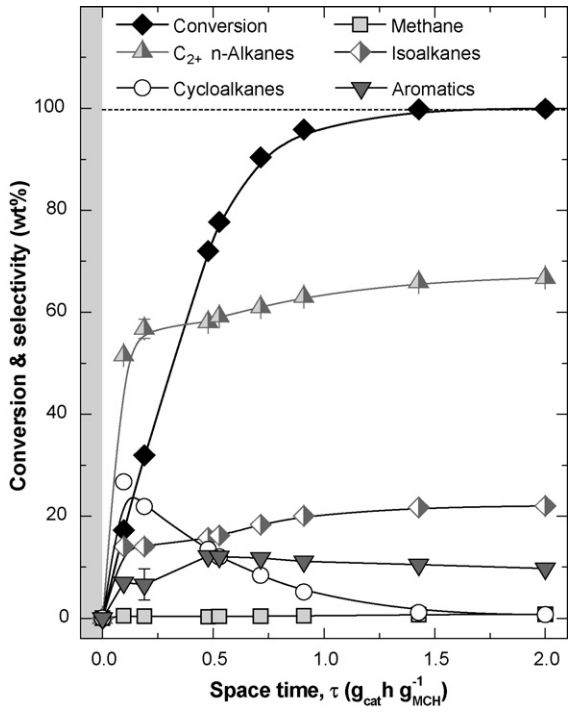

Fig. 3. Evolution of conversion and selectivity with space time. $P_{MCH} = 1$ bar, $P_{H_2} = 39$ bar, 350 °C.

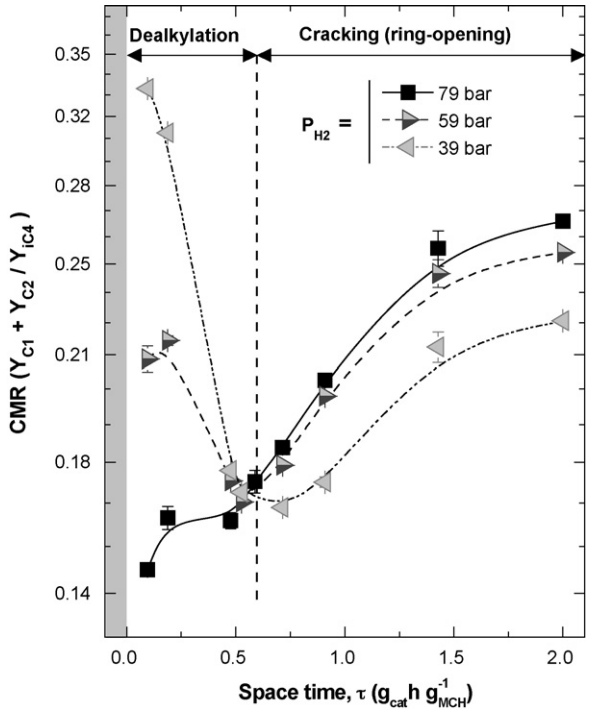

Fig. 4. Effect of hydrogen partial pressure on the evolution of CMR index (Eq. (1)). $P_{MCH} = 1$ bar, 350 °C.

is evidence of the high activity of the acid catalyst under the reaction conditions studied.

Furthermore, an increase in hydrogen partial pressure implies weakening the dehydrogenation steps responsible for aromatic formation. In this case, despite toluene is formed in a small amount, this react further over the HZSM-5 zeolite to form benzene and xylenes by disproportionation [23,24]. These results were confirmed previously for PyGas hydrodearomatization and required considering the hydrogen concentration in the differential rate equations of the kinetic model [25].

The evolution of MCH conversion and selectivity (or mass fraction of each product by mass unit of total products) with space time is shown in Fig. 3, using the following conditions: 350 °C and 40 bar. At the reactor inlet ($\tau < 0.1\ g_{cat}\ h\ g_{MCH}{}^{-1}$), two reactions of MCH transformation are combined: Isomerization and endocyclic cracking. Consequently, the selectivity to cycloalkanes (dimethyl-cyclopentane and ethyl-cyclopentane) and to alkanes increases very rapidly. When temperature is sufficiently high (as that corresponding to Fig. 3) the formation of *n*-alkanes is very rapid and, together with non-reacted MCH, they are the main components in the stream. The cycloalkanes coming from isomerization continuously undergo endocyclic scission up to a space time of $1.5\ g_{cat}\ h\ g_{MCH}{}^{-1}$, whereas the formation of aromatics by dehydrogenation peaks at $\tau = 0.5\ g_{cat}\ h\ g_{MCH}{}^{-1}$.

Although the yield of each lump does not change significantly for high space time values ($\tau > 1.0\ g_{cat}\ h\ g_{MCH}{}^{-1}$), under the conditions studied in Fig. 3, the average molecular weight of each lump does change as a consequence of secondary and tertiary cracking. Hence, methane selectivity increases as space time is increased, and this effect is more evident at higher temperatures (>350 °C) due to the enhanced dealkylation (also called exocyclic cracking) of alkylcycloalkanes and Haag-Dessau cracking. It is worth mentioning that the thermal cracking, responsible for the formation of methane under unit FCC conditions, has a very low impact on this formation in the present study [26,27].

In order to analyse the importance of Haag-Dessau cracking, Fig. 4 shows the evolution of CMR (calculated using Eq. (3)) with space time for different hydrogen partial pressures. This figure shows a high value of CMR index at lower space time values, which is more remarkable under low hydrogen partial pressures. This result confirms that the predominant reaction under low cycloalkane conversion is dealkylation of methyl- and ethyl-cycloalkanes to produce methane, ethane and non-substituted cycloalkanes via protolytic cracking (the intermediates required for β-scission to produce methane and ethane are very unstable). As hydrogen partial pressure is decreased, the dealkylation step is enhanced, as happens when temperature is decreased. The minimum in CMR shown in Fig. 4 (at $\tau = 0.6\ g_{cat}\ h\ g_{MCH}{}^{-1}$, specially for $P_{H_2} = 39$ bar) is a result of the maximum yield of isobutene. At space time values higher than $0.6\ g_{cat}\ h\ g_{MCH}{}^{-1}$, dealkylation is less important, due to the smaller concentration of cycloalkanes, and protolytic cracking and cracking by exocyclic scission are favoured (isobutane yield decrease as a results of its cracking). Thus, both mechanisms seem to be favoured in the cracking with hydrogen, given that carbonium ion formation is favoured and hydrogenation of alkanes formed by β-scission of carbenium ions activates this mechanism.

A further favourable circumstance of ring-opening with hydrogen is the insignificant deactivation of the catalyst by coke, which is a result of the hydrogenation of coke precursors and

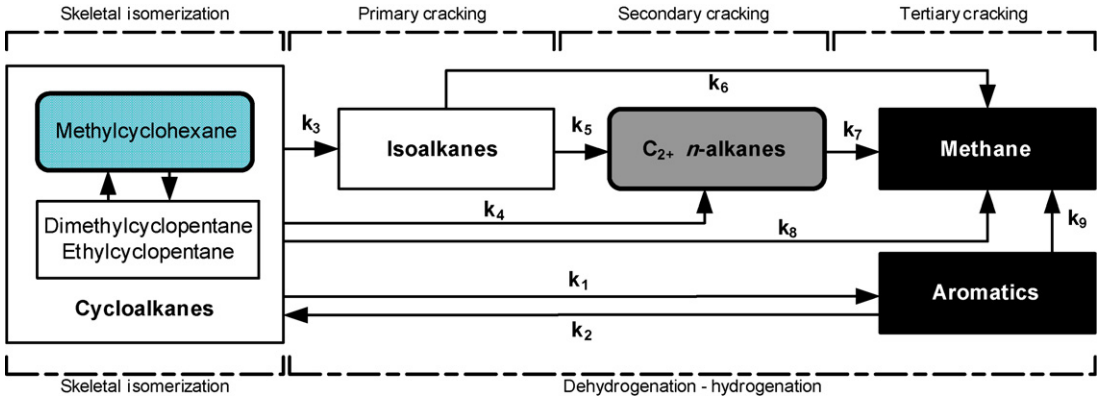

Fig. 5. Kinetic scheme proposed for the ring-opening of methylcyclohexane on HZSM-5 zeolite.

minimization of their condensation steps [28,29]. There is only slight deactivation under conditions of high temperature, low space time and low hydrogen partial pressure. Under these conditions, for the initial 2 h time-on-stream the small coke deposition affects the strongest acid sites of the catalyst. In order to avoid the effect of deactivation under these specific conditions, the experimental results used in the kinetic modelling have been obtained with the equilibrated catalyst, subsequent to this initial period of very low deactivation avoiding more severe conditions where coke formation is not neglectable and methane (inert during steam cracking and hence, a not desired product) yield is substantially higher.

3.2. Proposed kinetic model

The kinetic scheme proposed (Fig. 5) is based on the one proposed by Cerqueira et al. [11,12] and recently verified by Caeiro et al. [30] for MCH cracking without hydrogen. The steps of isomerization of cycloalkanes and disproportionation of aromatics were not considered in the model, as neither them takes part in the steps involved in the formation of isoalkanes and C_{2+} *n*-alkanes. This is based on the similar reactivity of cycloalkane isomers over the acid sites of the zeolite [31,32]. Furthermore, the lump of aromatics is made up of molecules that are very non-reactive due to their resonance energy.

The mass fraction of each lump in the kinetic model (x_i) has been taken as the variable to fit. This concentration is that corresponding to the whole stream, including hydrogen. The hydrogen mass fraction is calculated from the global mass balance, according to the initial partial pressure of this compound. The differential equations quantifying the mass fraction variation of each lump (Fig. 5) along the reactor are:

$$\frac{dx_C}{d\tau} = -k_1 x_C + k_2 x_A x_{H_2}^{\alpha} - k_3 x_C x_{H_2}^{\alpha} - k_4 x_C x_{H_2}^{\alpha} - k_8 x_C x_{H_2}^{\alpha} \quad (5)$$

$$\frac{dx_I}{d\tau} = k_3 x_C x_{H_2}^{\alpha} - k_5 x_I x_{H_2}^{\alpha} - k_6 x_I x_{H_2}^{\alpha} \quad (6)$$

$$\frac{dx_P}{d\tau} = k_4 x_C x_{H_2}^{\alpha} + k_5 x_I x_{H_2}^{\alpha} - k_7 x_P x_{H_2}^{\alpha} \quad (7)$$

$$\frac{dx_M}{d\tau} = k_6 x_I x_{H_2}^{\alpha} + k_8 x_C x_{H_2}^{\alpha} + k_9 x_A x_{H_2}^{\alpha} \quad (8)$$

$$\frac{dx_A}{d\tau} = k_1 x_C - k_2 x_A x_{H_2}^{\alpha} - k_9 x_A x_{H_2}^{\alpha} \quad (9)$$

where the subscripts correspond to: C: cycloalkanes; I: isoalkanes; P: paraffins or C_{2+} *n*-alkanes; M: methane; A: aromatics; H_2: hydrogen. The effect of hydrogen partial concentration in the rate expressions has been considered with an order (α). This value was initially considered as a fitting-parameter. The calculation has been carried out by reparameterization of Arrhenius equation in order to consider the effect of temperature in the kinetic constants.

3.3. Kinetic constants

The differential equations were initially solved as expressed in Eqs. (5)–(9), however k_2, k_7 and k_9 show no relevance (low significance) in the prediction of the reaction yields and conversion. The exclusion of these constants is also a consequence of the aforementioned results: (i) the rate of formation of cycloalkanes from aromatics (k_2) can be ignored; (ii) C_{2+} *n*-alkane protolytic scission to form methane (k_7) is neglectable at mild conditions; (iii) aromatic dealkylation (k_9) is not important as disproportionation of toluene to form benzene and xylenes is more favourable over an HZSM-5 zeolite (reaction not considered since it does not affect the global hydrogenation rate). According to these results, Table 1 summarizes the more significative kinetic constant values (k_1, k_3–k_6, k_8) at 390 °C, pre-exponential factors and the activation energies of the steps described in the reaction scheme (Fig. 5). The residual sum of squares of the regression (SSR) is 0.188 and the variance 1.49 10^{-4}. The value of the F (Fisher) sampling distribution for the global fitting is 576, and the critical value (Fc) is 2.18, at a 95% confidence interval.

The reaction order for hydrogen (α) was a fitting variable in the first calculations, then based on the trend in results, a value of $\alpha = 2$ has been taken, which simplifies the model and provides a physical meaning to it. Raiche et al. [7] demonstrated that at more elevated hydrogen concentration that the ones studied here (100 bar) the rate of ring-opening is decreased as a result of lowering the concentration of MCH inside the zeolitic pores.

Table 1
Kinetic parameters for ring-opening of MCH ($\alpha = 2$)

Reaction	$k_i^{390\,^\circ C}$		k_i^0	Ea_i (kJ/mol)
k_1	0.83 ± 0.03	$\frac{g_{hy}^{out}}{g_{cst} h}$	$(1.94 \pm 0.06)\ 10^{11}$	144 ± 3
k_3	8.9 ± 0.2	$\frac{(g_{hy}^{out})^3}{g_{H_2}^2 g_{cat} h}$	$(2.99 \pm 0.07)\ 10^{10}$	121 ± 1
k_4	25.3 ± 0.4	$\frac{(g_{hy}^{out})^3}{g_{H_2}^2 g_{cat} h}$	$(5.00 \pm 0.08)\ 10^{11}$	130 ± 1
k_5	0.38 ± 0.07	$\frac{(g_{hy}^{out})^3}{g_{H_2}^2 g_{cat} h}$	$(1.32 \pm 0.26)\ 10^{8}$	106 ± 4
k_6	0.07 ± 0.01	$\frac{(g_{hy}^{out})^3}{g_{H_2}^2 g_{cat} h}$	$(2.55 \pm 0.23)\ 10^{13}$	185 ± 6
k_8	0.24 ± 0.07	$\frac{(g_{hy}^{out})^3}{g_{H_2}^2 g_{cat} h}$	$(5.80 \pm 0.45)\ 10^{16}$	220 ± 9

The ring scission of cycloalkanes to produce C_{2+} *n*-alkanes (k_4) seems to be the fastest reaction at 390 °C, considering that under these conditions the predominant mechanism of cracking is the bimolecular one [15] and this route yields mainly isoalkanes (most stable intermediate carbocation during β-scission and isomerization). This result is a consequence of the lower activation energy during conversion of isoalkanes into C_{2+} *n*-alkanes (Ea_5) which leads to an apparent-faster k_4 reaction.

The apparent activation energies of the two steps which yield methane (Ea_6 and Ea_8) have the highest values among the reactions involved. Taking into account that methane is formed through protolytic cracking (no thermal cracking involved in our conditions), this result coincides with the general concern that monomolecular cracking has higher activation energy value compared to bimolecular cracking [14,33].

To proof whether the fitting is satisfactory and the kinetic model is able to faithfully predict the distribution of products in the whole range studied, Fig. 6 shows the results of the fitting (partition diagram) between the calculated and experimental concentrations for the lumps of the kinetic scheme in Fig. 5. According to this result the accuracy of the predicted values of concentrations appear greatly satisfactory.

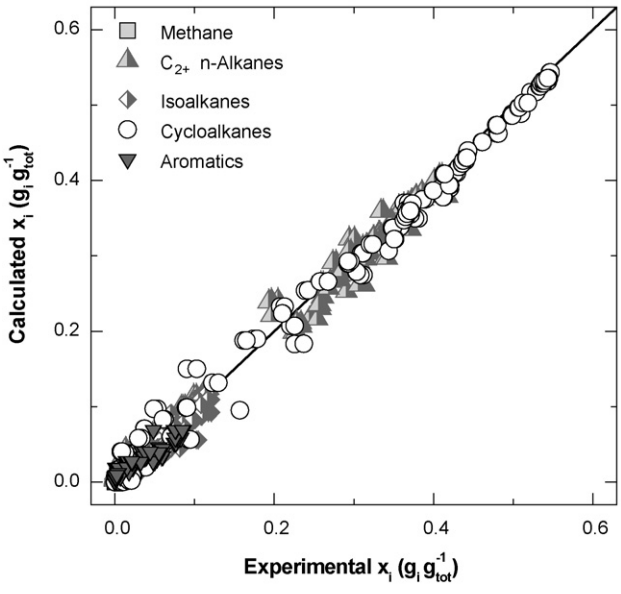

Fig. 6. Comparison of calculated and experimental results for the lump concentrations in the ring-opening of MCH.

3.4. Simulation of the reactor

The kinetic model obtained, from Eqs. (5)–(9) and the results summarized in Table 1, has been used in the simulation of the reactor (code in Matlab R14). Fig. 7 compares the results of stream composition (excluding hydrogen) calculated with the kinetic model provided with the parameters of best fitting (lines) and the experimental results (points). These results correspond to given experimental conditions (space time values in the 0–2 $g_{cat}\,h\,g_{MCH}^{-1}$ range, 400 °C and $P_{H_2} = 59$ bar) and are an example of the suitable fit in the whole range of experimental conditions used in this study.

Using the above-mentioned routine for simulation, maps of composition of the different lumps are obtained as a function of the experimental conditions. Fig. 8 corresponds to a map of space time–temperature when the remaining conditions are fixed to $P_{H_2} = 39$ bar, $P_{MCH} = 1$ bar. The optimal conditions aimed at the production of a synthetic steam cracker feedstock (high concentration of C_{2+} *n*-alkanes and low of methane and aromatics) are: ca. 420 °C and $\tau > 1.0\,g_{cat}\,h\,g_{MCH}^{-1}$, and when a suitable gasoline pool feedstock (mainly constituted by isoalkanes) is the target, the best conditions are: 340 °C and $\tau > 2.0\,g_{cat}\,h\,g_{MCH}^{-1}$.

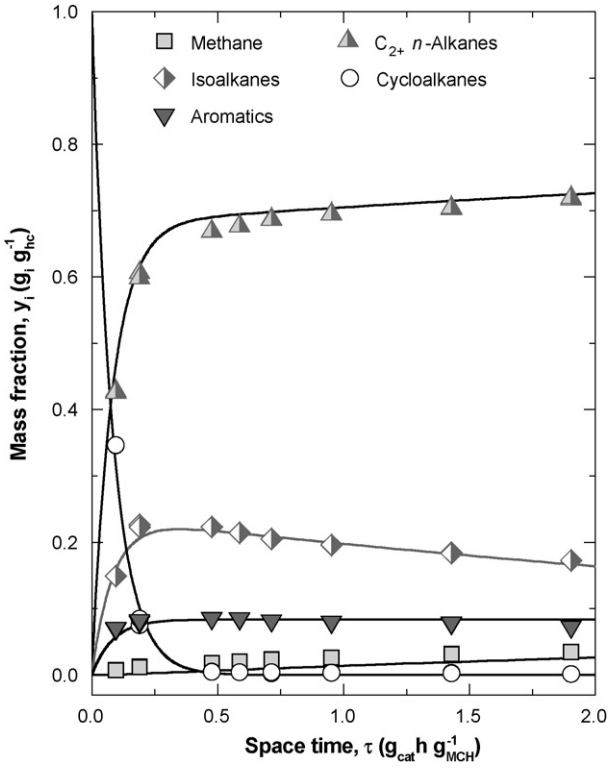

Fig. 7. Comparison of composition results (mass fraction in the hydrocarbon stream, excluding hydrogen) calculated using the kinetic model (lines) with the experimental ones (points). 400 °C, $P_{MCH} = 1$ bar and $P_{H_2} = 59$ bar.

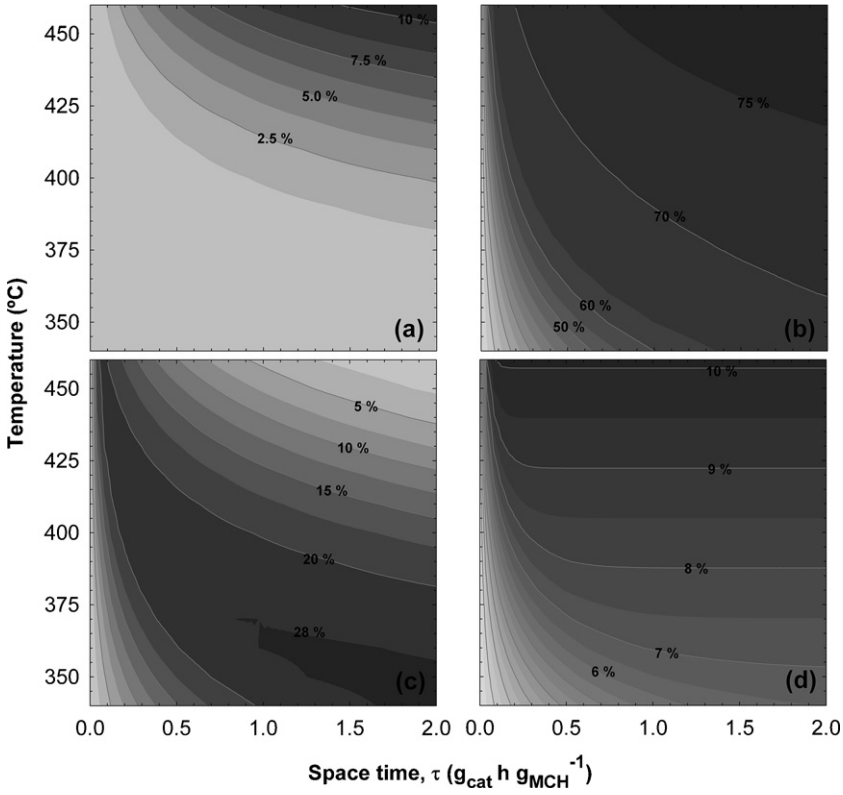

Fig. 8. Effect of temperature and space time on the composition (weight percent in the hydrocarbon stream; wt%) of the different *lumps*: Graph **a**, methane. Graph **b**, C_{2+} *n*-alkanes. Graph **c**, isoalkanes. Graph **d**, aromatics.

Moreover, the simulation allows for checking whether the model has the ability to faithfully predict the effects of process variables on MCH hydroconversion and selectivity, i.e. the experimental observations are described in the values of the constant. Hence the results of the constants given in Table 1 can be linked with: (i) methane is only formed only under high space time and temperature values (Fig. 8a). (ii) C_{2+} *n*-alkanes are produced mainly at low values of space time, especially at temperatures higher than 350 °C (Fig. 8b), and increasing the space time does not lead to a remarkable increase in C_{2+} *n*-alkane yield. (iii) Isoalkane concentration peaks at intermediate values of temperature and high values of space time (Fig. 8c). (iv) The aromatics are due to dehydrogenation by an irreversible and rapid reaction (Fig. 8d). At temperatures above 430 °C and space time values higher than 0.4 g_{cat} h $g_{MCH}{}^{-1}$, the concentration of aromatics remains constant along the reactor.

4. Conclusions

The kinetic model proposed for methylcyclohexane ring-opening over a HZSM-5 zeolite-based catalyst considers the particular circumstances in the cracking attributable to the high concentration of hydrogen in the reaction medium. Hydrogen concentration severely affects conversion and selectivity towards ring-opening products, due to the enhancement of both cracking mechanisms (classic β-scission and protolytic cracking) by the faster hydrogenation of the alkenes generated and by carbonium ions, respectively. Hence, hydrogen concentration has been considered in the individual cracking steps of the reaction scheme with a second order reaction.

It is noteworthy that kinetic model parameters have been obtained by operating in a wide range of experimental conditions and faithfully considering the particularities of the ring-opening in the presence of hydrogen process that occurs without deactivation by coke. Furthermore, the irrelevance of dealkylation–hydrogenation of aromatics and cracking of C_{2+} *n*-alkanes has been proven. Amongst the experimental observations in the ring-opening of MCH, the kinetic model proposed includes: (i) methane is formed only under severe conditions of temperature and space time; (ii) C_{2+} *n*-alkanes are formed for low values of space time and do not change significantly along the reactor at temperatures higher than 400 °C; (iii) the isoalkane yield reaches a maximum at intermediate temperatures and space time values; (iv) the formation of aromatics is rapid (for $\tau > 0.4$ h and 400 °C) and irreversible.

The model proposed is also valid as a basis for the kinetic modelling of ring-opening of more complex naphthenic feedstock, such as the streams obtained in the hydrogenation of pyrolysis gasoline (PyGas), light cycle oil (LCO) in FCC units or other refinery aromatic streams.

Acknowledgements

The authors gratefully acknowledge the valuable comments and suggestions made by L. Santamaria. This work has been carried out through the financial support of the Ministry of

Education and Science of the Spanish Government (Project PPQ2003-07822) and of the University of the Basque Country (Project 9/UPV 00069.310-13607/2001). P.C. wishes to thank the Basque Government (Dept. of Education, Universities & Research: BFI02.96) for the Fellowship.

References

[1] CEFIC, Cefic, Petrochemistry Activity Review, 2005.
[2] G.B. McVicker, M. Daage, M.S. Touvelle, C.W. Hudson, D.P. Klein, W.C. Baird, B.R. Cook, J.G. Chen, S. Hantzer, D.E.W. Vaughan, E.S. Ellis, O.C. Feeley, J. Catal. 210 (2002) 137–148.
[3] H.B. Du, C. Fairbridge, H. Yang, Z. Ring, Appl. Catal. A: Gen. 294 (2005) 1–21.
[4] J. Weitkamp, A. Raichle, Y. Traa, Appl. Catal. A: Gen. 222 (2001) 277–297.
[5] C. Ringelhan, G. Burgfels, J.G. Neumayr, W. Seuffert, J. Klose, V. Kurth, Catal. Today 97 (2004) 277–282.
[6] A. Raichle, M. Ramin, D. Singer, M. Hunger, Y. Traa, J. Weitkamp, Catal. Commun. 2 (2001) 69–74.
[7] A. Raichle, Y. Traa, J. Weitkamp, Appl. Catal. B: Environ. 41 (2003) 193–205.
[8] L.B. Galperin, J.C. Bricker, J.R. Holmgren, Appl. Catal. A: Gen. 239 (2003) 297–304.
[9] T. Sugii, Y. Kamiya, T. Okuhara, Appl. Catal. A: Gen. 312 (2006) 45–51.
[10] F. Figueras, B. Coq, C. Walter, J.Y. Carriat, J. Catal. 169 (1997) 103–113.
[11] H.S. Cerqueira, P. Magnoux, D. Martin, M. Guisnet, Abs. Pap. Am. Chem. Soc. 216 (1998) 835.
[12] H.S. Cerqueira, P.C. Mihindou-Koumba, P. Magnoux, M. Guisnet, Ind. Eng. Chem. Res. 40 (2001) 1032–1041.
[13] P.C. Mihindou-Koumba, H.S. Cerqueira, P. Magnoux, M. Guisnet, Ind. Eng. Chem. Res. 40 (2001) 1042–1051.
[14] S. Kotrel, H. Knozinger, B.C. Gates, Micropor. Mesopor. Mater. 35/36 (2000) 11–20.
[15] M. Stöcker, Micropor. Mesopor. Mater. 82 (2005) 257–292.
[16] P. Castaño, B. Pawelec, J.L.G. Fierro, J.M. Arandes, J. Bilbao, Appl. Catal. A: Gen. 315 (2006) 101–113.
[17] A.T. Aguayo, A.G. Gayubo, J. Erena, M. Olazar, J.M. Arandes, J. Bilbao, J. Chem. Technol. Biotechnol. 60 (1994) 141–146.
[18] A.G. Gayubo, P.L. Benito, A.T. Aguayo, M. Olazar, J. Bilbao, J. Chem. Technol. Biotechnol. 65 (1996) 186–192.
[19] S. Sanchez, M.A. Rodriguez, J. Ancheyta, Ind. Eng. Chem. Res. 44 (2005) 9409–9413.
[20] J. Ancheyta, S. Sanchez, M.A. Rodriguez, Catal. Today 109 (2005) 76–92.
[21] O. Cairon, K. Thomas, A. Chambellan, T. Chevreau, Appl. Catal. A: Gen. 238 (2003) 167–183.
[22] A.F.H. Wielers, M. Vaarkamp, M.F.M. Post, J. Catal. 127 (1991) 51–66.
[23] M.A. Uguina, J.L. Sotelo, D.P. Serrano, Appl. Catal. 76 (1991) 183–198.
[24] L.Y. Fang, S.B. Liu, I. Wang, J. Catal. 185 (1999) 33–42.
[25] P. Castano, B. Pawelec, J.L.G. Fierro, J.M. Arandes, J. Bilbao, Fuel 86 (2007) 2262–2274.
[26] S.J. Buchanan, Y.G. Adewuyi, Appl. Catal. A: Gen. 134 (1996) 247–262.
[27] J.M. Arandes, I. Abajo, I. Fernández, M.J. Azkoiti, J. Bilbao, Ind. Eng. Chem. Res. 39 (2000) 1917–1924.
[28] A.T. Aguayo, P.L. Benito, A.G. Gayubo, M. Olazar, J. Bilbao, Stud. Surf. Sci. Catal. 88 (1994) 567–572.
[29] M. Guisnet, P. Magnoux, Appl. Catal. A: Gen. 212 (2001) 83–96.
[30] G. Caeiro, P. Magnoux, J.M. Lopes, F. Lemos, F.R. Ribeiro, J. Mol. Catal. A: Chem. 249 (2006) 149–157.
[31] F. van Landeghem, D. Nevicato, I. Pitault, M. Forissier, P. Turlier, C. Derouin, J.R. Bernard, Appl. Catal. A: Gen. 138 (1996) 381–405.
[32] G.G. Martens, G.B. Marin, AIChE J. 47 (2001) 1607–1622.
[33] A. Raichle, Y. Traa, F. Fuder, M. Rupp, J. Weitkamp, Angew. Chem. Int. Ed. 40 (2001) 1243–1246.